Band offsets and strain in CdTe-GaAs heterostructures

G. Bratina, L. Sorba,* A. Antonini, G. Ceccone, R. Nicolini, G. Biasiol, and A. Franciosi
Laboratorio Tecnologie Avanzate Superfici e Catalisi del Consorzio Interuniversitario di Fisica della Materia, Area di Ricerca, Padriciano 99, I-34012 Trieste, Italy
and Department of Chemical Engineering and Materials Science, University of Minnesota, Minneapolis, Minnesota 55455

J. E. Angelo and W. W. Gerberich
Department of Chemical Engineering and Materials Science, University of Minnesota, Minneapolis, Minnesota 55455
(Received 3 November 1992; revised manuscript received 15 April 1993)

CdTe(111)-GaAs(001) and CdTe(001)-GaAs(001) heterostructures were synthesized through molecular-beam epitaxy. *In situ* monochromatic x-ray photoemission spectroscopy and reflection high-energy electron diffraction, together with *ex situ* cross-sectional transmission electron microscopy, were exploited to probe the relation between overlayer orientation, residual strain, and the band discontinuities. CdTe(001)-GaAs(001) heterostructures appear fully relaxed even at the lowest overlayer thicknesses explored through the formation of a misfit dislocation network. Correspondingly, the valence-band maximum in the CdTe(001) overlayer is found 0.07–0.09 eV *below* that of GaAs(001). In CdTe(111)-GaAs(001) heterostructures, we find that residual strains are gradually accommodated within a 200-Å-thick CdTe layer near the interface. The average position of the valence-band maximum in CdTe(111) is 0.09–0.11 eV *above* that of GaAs(001) at the interface. The difference in valence-band discontinuity for the two interfaces is qualitatively consistent with that expected from the effect of the residual strain on the valence-band maximum of CdTe(111).

I. INTRODUCTION

Heterovalent semiconductor heterostructures, i.e., heterostructures comprised of semiconductors of different chemical valence, are gaining attention because of their potential use in optoelectronic devices and in connection with the integration of optical detectors and emitters with Si- or GaAs-based high-speed signal processing circuits.[1–4] The properties of such heterostructures, however, are less well known than those of isovalent systems such as AlAs-GaAs and far more difficult to model theoretically. The cancellation of systematic errors that may occur in electronic-structure calculations is generally less effective when the two semiconductors involved exhibit different valence, electronegativity, and charge distribution.[5,6] Recent linear-response theory results indicate that while in isovalent heterostructures the band offsets should depend only on the bulk properties of the two semiconductors comprising the junction,[7] at polar interfaces between heterovalent semiconductors the offsets may depend on the details of the interface, including crystallographic orientation and atomic reconstruction.[8,10–12]

The sensitivity of heterojunction parameters to the local interface environment makes such systems good candidates for heterojunction engineering,[13–16] with the goal of optimizing the band offsets to a given device application, but complicates comparison between theory and experiment. The local dipole and strain-related contributions to heterostructure properties are also difficult to evaluate in the local-density functional framework for heterovalent systems,[17] and the fact that the individual element comprising each type of semiconductor act as dopants in the other type of semiconductor poses additional questions about the electrostatic and composition profile that can be obtained in practice.

We selected the CdTe-GaAs system as a prototype II-VI/III-V heterovalent heterojunction on two accounts. First, a large body of structural data is available for this system, including extensive transmission electron microscopy and grazing incidence x-ray diffraction (XRD) studies. Second, this system offers the unique opportunity of varying interface crystallographic orientation and strain and examining the corresponding variation in the band discontinuities. CdTe growth on GaAs(001) surfaces is initiated by the adsorption of Te atoms[18] and can proceed with (111) or (001) orientation depending on the initial Te-GaAs(001) configuration. The (111)- and (001)-oriented interfaces are substantially different in terms of dangling-bond density, strain, and atomic structure,[19–21] and should therefore exhibit different thermodynamic stability.[22]

We synthesized the two types of interfaces by molecular-beam epitaxy (MBE) of CdTe on MBE-grown GaAs buffer layers. We discuss here studies of the interface atomic structure by reflection high-energy electron diffraction (RHEED) and cross-sectional transmission electron microscopy (XTEM), in parallel with *in situ* studies of the band offsets by means of monochromatic x-ray photoemission spectroscopy (XPS).

II. EXPERIMENTAL DETAILS

All heterostructures were fabricated by solid source MBE in a facility consisting of a Riber 32*P* MBE chamber for GaAs growth, a similar chamber for the

growth of CdTe, and an analysis chamber equipped with a small spot monochromatic XPS, all interconnected through an ultrahigh vacuum transfer line. The XPS spectrometer employs Al $K\alpha$ radiation (1486.6 eV) monochromatized and focused by a bent crystal monochromator and a hemispherical electrostatic electron energy analyzer with an overall energy resolution (electrons plus photons) of 0.75 eV. Photoelectrons are collected at an average takeoff angle of 55° from the sample normal, so that the effective escape depth is 15 Å.[23]

GaAs(001) semi-insulating wafers were etched in a $2H_2O_2$:$5NH_4OH$:$10H_2O$ solution and preheated in UHV at 300 °C. It has been found that CdTe nucleation on GaAs proceeds initially by the adsorption of submonolayer or monolayer coverages of Te.[2] CdTe film orientation is affected by such factors as substrate temperature and As pressure, which can both change the GaAs(001) surface reconstruction, and by the Te coverage and the Te-induced surface reconstruction. The effects of these parameters on film orientation has been summarized in a precursor surface phase diagram.[24] Growth of (001)-oriented overlayers occurs with epitaxial relations (001)CdTe||(001)GaAs and $[1\bar{1}0]$CdTe||[110]GaAs and a 14.6% compressive misfit.[18] (111)-oriented growth occurs with epitaxial relations $[11\bar{2}]$CdTe||[110]GaAs and $[1\bar{1}0]$CdTe||$[1\bar{1}0]$GaAs. The resulting anisotropic misfit is +0.65% (tensile) in the $[11\bar{2}]$CdTe||[110]GaAs direction and −14.6% (compressive) in the $[1\bar{1}0]$CdTe||$[1\bar{1}0]$GaAs direction. In addition, two different orientations of CdTe(111) with respect to the $(1\bar{1}0)$ plane of GaAs (related by a rotation of π about the [001] direction) can coexist on a single substrate, and their junctions define twin boundaries.[18]

CdTe(111) layers were obtained with a two-stage III-V/II-VI growth procedure. After GaAs oxide removal at 580 °C under As_4 flux, a 1-μm-thick nominally undoped or n^+ (Si-doped $n=5\times10^{18}$ cm^{-3}) GaAs(001) substrate layer exhibiting the As-stabilized 2×4 reconstruction was grown at the same temperature in the III-V growth chamber. The background doping of the nominally undoped layers was p type with $p\approx8\times10^{14}$ cm^{-3}, as determined by resistivity and Hall measurements at 77 K. The sample was then transferred to the II-VI growth chamber where two effusion cells were employed, one containing elemental Te and one containing compound CdTe. The initial GaAs(001) As-rich $c(4\times4)$ surface, obtained upon cooling the substrate under As_4 flux in the III-V chamber prior to transfer, was exposed to a Te_2 flux with beam equivalent pressure $p=1\times10^{-6}$ Torr. Beam equivalent pressures were measured by exposing a nude ion gauge mounted on the substrate holder to the molecular beam. Upon disappearance of the RHEED pattern due to Te adsorption, the substrate temperature was increased at a rate of 5 °C/min to 340 °C. After a 6×1 reconstruction was observed,[25] the sample temperature was lowered to 290 °C and deposition of CdTe(111) was performed from a single effusion cell ($p=1\times10^{-6}$ Torr). The RHEED pattern in the [110] azimuth changed within a few seconds from $6\times$ to $1\times$ and exhibited the threefold symmetry characteristic of the CdTe(111) surface unit cell, upon rotation about the [111] axis.

CdTe(001) layers were obtained using two different procedures. In the first procedure, CdTe(001) layers were fabricated on ~0.5-μm-thick undoped GaAs(001) epitaxial layers grown in the III-V growth chamber and transferred to the II-VI growth chamber. Upon heating at 650 °C the excess arsenic was desorbed to yield the Ga-stabilized 3×1 RHEED pattern. The shutter of the compound CdTe cell was opened ($p=2.2\times10^{-7}$ Torr) and the temperature allowed to drop. At approximately 550 °C a 2×1 Te-induced surface reconstruction was observed. This pattern became spotty near the final growth temperature of 290 °C, to sharpen again after growth of 500–700 Å of CdTe. This procedure will be denoted in the text as procedure I.

A second procedure did not involve epitaxial growth of GaAs films. The GaAs(001) wafers were simply heated at 580 °C to remove the oxide and left at the same temperature for an additional 2 min. During that time the RHEED pattern changed from the 2×4 symmetry characteristic of the As-stabilized surface to the 3×1 periodicity characteristic of the Ga-rich surface.[26] The CdTe shutter was then opened and the sample cooled down rapidly under a CdTe flux.[21,27] A Te-induced 6×1 reconstruction was immediately observed.[25] At a substrate temperature of 320 °C the RHEED pattern became spotty and converged to a sharp 2×1 pattern after deposition of about 500–700 Å of CdTe. This growth protocol will be denoted in what follows as type II.

Growth rate and possible atomic intermixing across the interfaces were monitored using the integrated emission intensity and line shape of the Ga and Cd core levels as a function of CdTe deposition. Measurement of the Ga $3d$ core-level attenuation as a function of CdTe deposition yielded an exponential behavior with attenuation length of 15.3±1.1 Å. The corresponding increase in the Cd $4d$ emission followed a complementary exponential behavior with characteristic length of 14.2±1.2 Å. Within experimental uncertainty, this is the behavior expected for layer-by-layer growth in the absence of interdiffusion.[28] The line shape of the core levels [full width at half maximum (FWHM) of 1.10±0.05, 1.22±0.05, and 1.36±0.05 eV for the Ga $3d$ and Cd $4d$ doublets and the Ga $2p_{3/2}$ singlet, respectively] remained essentially unchanged at all stages of heterojunction fabrication. This also argues against chemical reaction at the interface.

We caution the reader that, although the above results can be used to rule out extensive atomic intermixing at the interfaces, based on XPS alone it is impossible to rule out intermixing at or below the atomic percent level. In the absence of interdiffusion, the attenuation of the substrate core emission can be used to gauge the overlayer thickness. The resulting calibration of the CdTe growth rate was confirmed by two different methods. RHEED intensity oscillations were monitored during growth of CdTe(001) on CdTe(001) using the same CdTe flux employed during the early growth stage on GaAs(001).[29] Also, *ex situ* profilometer measurements of thick CdTe films on GaAs were systematically performed. All rate calibration methods gave consistent results within an experimental uncertainty <13%. Typical growth rates em-

ployed were in the 1-Å/s range.

The structural quality of the interface and the amount of residual strain was examined *ex situ* by means of high-resolution XTEM. CdTe epitaxial layers ~ 0.6 μm thick were grown on GaAs(001) using the above growth procedures to obtain pure (111) or (001), as indicated by RHEED. The samples were prepared for XTEM observations by cutting and polishing to approximately 30 μm thickness using diamond paper. The samples were then argon-ion milled at liquid-nitrogen temperatures to electron transparency. The XTEM observations were performed in a Phillips CM30 transmission electron microscope operating at 300 kV and a JEOL 4000EX transmission electron microscope operating at 400 kV.

The heterojunction valence-band offsets were determined *in situ* by XPS for over 20 CdTe(111)-CdTe(001) and 15 CdTe(001)-GaAs(001) heterostructures involving 10–30-Å-thick CdTe layers with purely (111) or (001) symmetry, as indicated by the RHEED pattern. As in most photoemission studies,[30] the valence-band offset ΔE_v was obtained from the position of characteristic overlayer and substrate core level at the interface and the binding energy of the same core levels in appropriate bulk standards. We denote as E_b(Ga) and E_b(Cd) the positions of the Ga 3*d* and Cd 4*d* (or 3*d*) core levels relative to the Fermi level E_F in CdTe and GaAs standards with orientation and strain representative of those of the materials comprising the heterostructure. The corresponding positions of the valence-band maxima in the two standards are indicated as E_v(GaAs) and E_v(CdTe). Using, for example, the Cd 4*d* and Ga 3*d* core levels, for the valence-band offset we write

$$\Delta E_v = [E_b(\text{Ga } 3d) - E_v(\text{GaAs})] - [E_b(\text{Cd } 4d) - E_v(\text{CdTe})] + \Delta E_{\text{cl}} \quad (1)$$

where ΔE_{cl} is the measured core separation E_i(Cd 4*d*)$-E_i$(Ga 3*d*) at the interface and the positive sign in the offset puts the valence-band maximum in the overlayer below that of the substrate.[31] We emphasize that residual strains may in principle affect the measured binding energy of core levels relative to the valence maximum,[32–35] so that determination of the strain configuration in the different materials may be essential to correctly determine the heterojunction band discontinuities.

In principle overlayer or substrate doping resulting from interdiffusion below the sensitivity of XPS analysis could affect band bending and could change the apparent core-level separation if the semiconductor Debye length was to become comparable with the photoemission sampling depth. However, the corresponding expected changes in core separation, linewidths, and asymmetries with coverage are not observed in our results, suggesting that the Debye length remains longer than the XPS sampling depth. For example, our results show that the Cd 4*d*–Ga 3*d* energy distance remains at the value 8.30 ± 0.03 eV for CdTe(111) coverages in the 10–25-Å range. The corresponding value for the CdTe(001)-GaAs(001) case is 8.22 ± 0.03 eV. The line shapes of the corresponding core levels show no change throughout this stage of heterojunction fabrication.

The position of the valence-band maximum in the valence-band spectra was determined through a least-squares fit of the leading valence-band edge to suitably broadened theoretical density of states (DOS) for CdTe and GaAs,[36] i.e., through a method introduced several years ago by Grant and co-workers.[37,38] In this procedure the fitting parameters are the relative position and amplitude of the theoretical and experimental curves.

Two aspects that may substantially affect the result of the procedure are the width of the energy window in which to perform the least-squares minimization and the width of the broadening function. The former is necessarily limited by the difference in photoemission cross section for the different bands, which is not included in the theoretical curve. The best that can be expected is to find a range of window sizes in which the variation of the cross section is relatively small, so that the result of the fit is independent of window size. The latter accounts for the experimental resolution and can be determined through the line-shape analysis of a suitable core emission from a chosen standard sample.[37] Photoelectron energy distribution curves (EDC's) for the core emissions were least-squares fitted to a superposition of Lorentzian and Gaussian functions. The width of the Lorentzian function is related to the intrinsic lifetime broadening and the full width at half maximum σ of the Gaussian function represents the width of the spectrometer response function.

We obtained σ through three different measurements. First, we determined the FWHM of the Au $4f_{7/2}$ core-level emission from a gold standard (FWHM of 0.84 ± 0.01 eV). After deconvolution of a lifetime-related Lorentzian contribution (FWHM of 0.317 ± 0.010 eV, from Ref. 39) to the overall line shape we found $\sigma = 0.72 \pm 0.01$ eV. Second, a least-squares fit of the Ga 3*d* spin-split doublet in the standard in terms of Gaussian and Lorentzian contributions yielded $\sigma = 0.79 \pm 0.01$ eV. Finally, we determined the width of the Fermi level in the valence-band EDC's from a polycrystalline Mo standard cleaned *in situ*, and found $\sigma = 0.73 \pm 0.05$ eV. We selected an average value $\sigma = 0.75$ for the broadening parameter.

III. RESULTS

A. Atomic structure

Despite the large lattice mismatch between CdTe and GaAs, and the different competing surface reconstructions that may result in multiple domains,[40–43] both our RHEED and XTEM results emphasize the high degree of long-range order that can be achieved near the interface with a suitable growth protocol. RHEED results for CdTe(111)-GaAs(001) interfaces are shown in Figs. 1(a) and 1(b); the corresponding results for CdTe(001)-GaAs(001) interfaces are shown in Figs. 1(c) and 1(d).

1. CdTe(001)-GaAs(001)

In Fig. 1(c) we show a representative 10-keV RHEED pattern[44,45] observed in the [110] GaAs azimuth from a

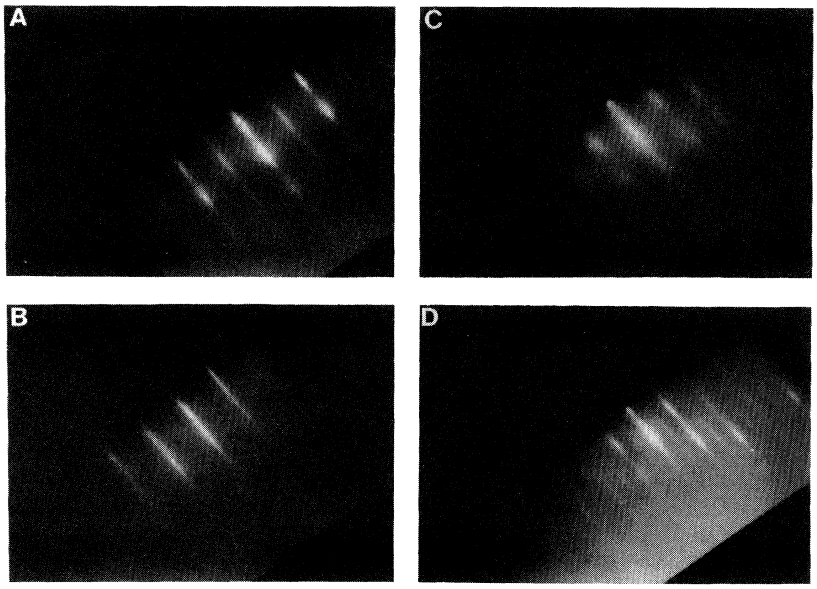

FIG. 1. (a) Reflection high-energy electron diffraction (RHEED) pattern at 10 keV from a 13-Å-thick CdTe(111) epitaxial layer grown by molecular-beam epitaxy (MBE) at 330 °C on a 1-μm-thick undoped GaAs(001) 2×4 buffer layer. The GaAs buffer was grown by MBE at 580 °C on GaAs(001). Azimuth: [$1\bar{1}0$]GaAs. (b) RHEED pattern from a 0.6-μm-thick CdTe(111) epitaxial layer grown in the same conditions as in (a). (c) RHEED pattern from a 14-Å-thick CdTe(001) epitaxial layer grown at 330 °C on a GaAs(001) wafer after oxide desorption at 580 °C and exposure to a suitable Te flux. Azimuth: [110]GaAs. (d) RHEED pattern for a 0.6-μm-thick CdTe(001) epitaxial layer grown in the same conditions as in (c).

14-Å-thick CdTe(001) layer deposited on an etched and deoxidized GaAs(001) wafer (procedure II). We show in Fig. 1(d) the $2\times$ pattern observed in the same azimuth from a 0.6-μm-thick CdTe(001) layer grown in the same conditions. The comparison between Figs. 1(c) and 1(d) qualitatively illustrates the structural quality of the CdTe(001)-GaAs(001) interface region for the heterostructures synthesized on deoxidized GaAs(001) wafers. Although the RHEED pattern, obtained on a 13-Å-thick CdTe(001) [Fig. 1(c)], shows indications of three-dimensional growth, the long-range periodicity is well defined and the lattice parameter homogeneous with that of the thicker sample (Fig. 1(d)).

In Fig. 2 we show high-resolution transmission electron micrographs of the interface region within CdTe-GaAs heterostructures, imaged along the [110] direction of GaAs. The length of the horizontal marker in Fig. 2(b) corresponds to 25 Å, and the magnification is the same in the two micrographs. The topmost section of each image corresponds to the MBE-grown CdTe overlayer, the bottom-most section to the MBE-grown GaAs substrate. Figure 2(a) was obtained from a 0.5-μm-thick CdTe(001) overlayer grown on a GaAs(001) buffer (procedure I). For the CdTe(001)-GaAs(001) heterostructure in Fig. 2(a), viewed along [$1\bar{1}0$]CdTe$||$[110]GaAs, the overlayer is fully relaxed and the -14.6% mismatch is accommodated through the formation of a network of misfit dislocations spaced 32 Å apart along the interface.[27,43] The vertical arrow marks the position of the core of one such dislocation.

2. *CdTe(111)-GaAs(001)*

In Fig. 1(a) we show a representative 10-keV RHEED pattern[45] from a 13-Å-thick CdTe(111) layer on GaAs, in the [$1\bar{1}0$]GaAs ($1\times$) azimuth. For comparison in Fig. 1(b) we show the pattern obtained in the same azimuth from a 0.6-μm-thick CdTe(111) layer on GaAs.

XTEM results obtained from a 0.5-μm-thick

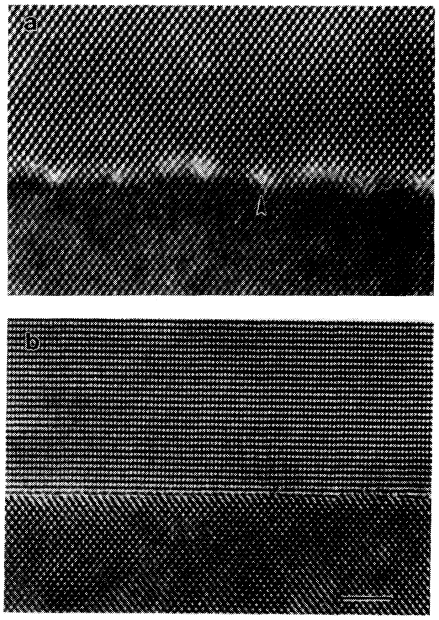

FIG. 2. High-resolution transmission electron micrographs of the interface region within CdTe-GaAs heterostructures, imaged along the [110] direction of GaAs. The length of the horizontal marker (horizontal bar, lower photograph) corresponds to 25 Å. The topmost section of each photograph corresponds to the MBE-grown CdTe overlayer, the bottom-most section of the MBE-grown GaAs substrate. (a) CdTe(001)-GaAs(001) heterostructure, viewed along [$1\bar{1}0$]CdTe$||$[110]GaAs. The overlayer is fully relaxed and the 14.6% mismatch is accommodated through the formation of a network of misfit dislocations spaced 32 Å apart along the interface. The vertical arrow marks the position of the core of one such dislocation. (b) CdTe(111)-GaAs(001) heterostructure, viewed along [$11\bar{2}$]CdTe $||$[110]GaAs. The overlayer in-plain strain configuration is inhomogeneous, in view of the -14.6% mismatch along [$1\bar{1}0$]CdTe$||$[$1\bar{1}0$]GaAs and the $+0.65\%$ mismatch along [$11\bar{2}$]CdTe$||$[110]GaAs.

CdTe(111) overlayer grown on a GaAs(001) buffer are shown in Fig. 2(b). For CdTe(111)-GaAs(001) the overlayer in-plain strain configuration is inhomogeneous, in view of the -14.6% mismatch along $[1\bar{1}0]$CdTe $||[1\bar{1}0]$GaAs and the $+0.65\%$ mismatch along $[11\bar{2}]$CdTe$||[110]$GaAs. In Fig. 2(b) the interface is viewed along $[11\bar{2}]$CdTe$||[110]$GaAs, and partial lattice relaxation of the large compressive mismatch can be gauged in the image by counting the number of CdTe-related lattice fringes per unit length. Within ~ 60 Å from the interface, the observed number of fringes is consistent with a constant residual strain $\varepsilon_{\parallel}[1\bar{1}0] \sim -1.4 \pm 0.3\%$. The strain gradually decreases with increasing distance from the interface and at about 130 Å is reduced to only $-0.4 \pm 0.3\%$. The observed residual strain at different distances from the interface is tabulated in the second column of Table I. In the perpendicular direction, the much smaller ($+0.65\%$) tensile mismatch is at least partially relaxed through the formation of rotational twins. This is shown in Fig. 3, in which a lower magnification transmission electron micrograph of the CdTe(111)-GaAs(001) heterostructure viewed along $[1\bar{1}0]$CdTe$||[1\bar{1}0]$GaAs explores extended regions of substrate and overlayer. A distribution of rotational twins in the $[11\bar{2}]$CdTe$||[110]$GaAs direction gradually accommodates the residual strain at the interface. An estimate of the residual strain in the overlayer in this direction could in principle be made from the average distance of the rotational twins in the direction parallel to the interface. Such an estimate of $\varepsilon_{\parallel}[11\bar{2}]$, however, would carry a substantial uncertainty because of the difficulty of acquiring a meaningful statistical sample of the number and distance of the rotational twins, and will not be discussed here.

Our XTEM-derived estimates of $\varepsilon_{\parallel}[1\bar{1}0]$ in CdTe(111)-GaAs(001) can be compared with grazing incidence XRD results in the literature for CdTe(111) thin films on GaAs(001).[40,46] For convenience, the XRD-derived residual strains are listed in column four of Table I as a function of the thickness of the CdTe overlayer. We emphasize that XTEM- and XRD-derived values of the residual strain correspond to physically different situations. The XTEM-derived values have been determined for a buried interface, as a function of the distance from the interface plane, and carry an uncertainty of ± 0.03. The XRD-determined strains are, instead, average values over the entire thickness of the thin film considered. The growth parameters employed were also somewhat different in the two cases. In view of such differences, the similarity between the XTEM- and XRD-derived values of the strain in Table I is quite compelling. We conclude that the situation observed during CdTe(111) thin-film growth is quite similar to the situation frozen in place near the buried interface. The residual strain profile is

TABLE I. Comparison of experimental residual strains in epitaxial CdTe(111) on GaAs(001), as determined from cross-sectional high-resolution transmission microscopy (XTEM) of 0.5-μm-thick CdTe overlayer (columns 1 and 2) grown by molecular-beam epitaxy (MBE) on GaAs(001) buffers (this work) and by grazing incidence x-ray diffraction (XRD) of CdTe thin films (columns 3 and 4) grown by MBE on chemically etched and thermally deoxidized GaAs(001) wafers (from Ref. 55). Column 1: distance from the interface plane in the XTEM micrographs. Column 2: residual strain in the direction parallel to $[1\bar{1}0]$GaAs, from XTEM. Column 3: thickness of the thin film examined by XRD. Column 4: residual strain in the direction parallel to $[1\bar{1}0]$GaAs, from XRD.

d (Å)	$10^{-2}\times\varepsilon_{\parallel}[1\bar{1}0]$	t (Å)	$10^{-2}\times\varepsilon_{\parallel}[1\bar{1}0]$
18.7	-1.43	20	-2.3
59.8	-1.43	35	-2.2
93.5	-0.73	50	-2.3
127.2	-0.38	100	-0.7

FIG. 3. Lower magnification high-resolution transmission electron micrograph of CdTe(111)-GaAs(001) heterostructure showing extended regions of substrate and overlayer along $[1\bar{1}0]$CdTe$||[1\bar{1}0]$GaAs. A distribution of rotational twins in the $[11\bar{2}]$CdTe$||[110]$GaAs direction gradually accommodates the residual strains at the interface.

relatively constant within the first 50–60 Å of CdTe, and then decreases quite rapidly at higher distances or thicknesses. In the perpendicular direction, the XRD results suggest that the small tensile strain is fully relaxed within 100 Å of the interface.[46]

B. Band offsets

1. CdTe(001)-GaAs(001)

XPS measurements of the valence-band offsets for CdTe(001)-GaAs(001) are simplified by the fully relaxed nature of CdTe(001) overlayer even at the relatively low thicknesses employed in the photoemission measurements. Representative results of XPS measurements of the valence-band offsets for CdTe(001)-GaAs(001) heterostructures are illustrated in Fig. 4. Heterojunctions obtained through procedures I and II were studied with consistent results. In the inset, we show EDC's for the valence-band emission from a 0.5-μm-thick CdTe(001) layer grown at 290 °C on a GaAs buffer (top) and from the GaAs(001) buffer (bottom). The zero of the binding energy scale corresponds to the valence-band maximum E_v for each sample. The location of E_v was determined from a least-squares fit[37,47] of the EDC's to a suitably broadened theoretical DOS (Ref. 36) in the region of the leading valence-band edge.

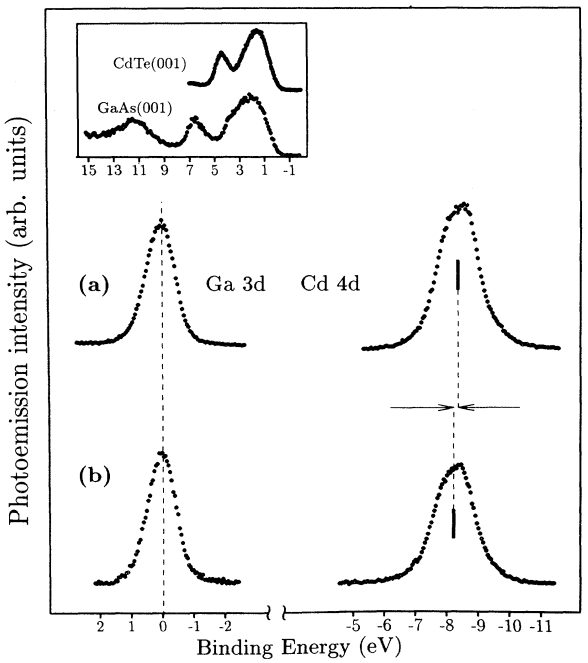

FIG. 4. Inset: valence-band emission from a 0.5-μm-thick CdTe(001) layer grown on GaAs(001) and a 1-μm-thick GaAs(001) buffer (bottom). The binding-energy scale for each sample was referenced to the valence-band maximum E_v as derived from a least-squares fit to a suitably broadened theoretical density of states. (a) Ga 3*d* and Cd 4*d* core-level emission from the same samples. Individual core binding energies were measured relative to the position of E_v in each sample. The zero of the binding energy scale is shown at the position of the Ga 3*d* centroid in GaAs, so that the apparent core-level separation is that expected in a hypothetical CdTe(001)-GaAs(001) heterojunction with zero valence-band offset. (b) Ga 3*d* and Cd 4*d* core emission from an actual CdTe(001)-GaAs(001) heterojunction fabricated by depositing a 15-Å-thick CdTe(001) layer on GaAs(001). The change in core-level separation relative to (a) gives directly the valence-band offset $\Delta E_v = +0.07 \pm 0.07$ eV. A similar value ($+0.09 \pm 0.07$ eV) was obtained using the Cd 3*d* core levels.

From the fitting procedure, we found[48] [see Eq. (1)]

$$E_b(\text{Ga } 3d) - E_v(\text{GaAs}) = 18.84 \pm 0.03 \text{ eV} ,$$

$$E_b(\text{Cd } 4d) - E_v(\text{CdTe}) = 10.54 \pm 0.03 \text{ eV} ,$$

$$E_b(\text{Cd } 3d) - E_v(\text{CdTe}) = 404.59 \pm 0.03 \text{ eV} ,$$

where the quoted uncertainty is the standard deviation of the values measured from 9 (GaAs) and 11 (CdTe) standards. The Ga 3*d* and Cd 4*d* core-level emission from the same two CdTe and GaAs standards is shown in Fig. 4(a). The position of each core level was determined relative to E_v in the corresponding sample (see inset), and the EDC's are plotted in Fig. 4(a) with the zero of the energy scale at the position of the Ga 3*d* centroid. The energy separation of the two core levels in Fig. 4(a) is therefore that expected from a hypothetical CdTe(001)-GaAs(001) heterojunction with zero valence-band offset.

Representative EDC's for the Ga 3*d* and Cd 4*d* core-level emission from a CdTe(001)-GaAs(001) heterostructure are shown in Fig. 4(b), with the binding energy scale again referred to the Ga 3*d* centroid. The data shown are for a CdTe overlayer thickness of 15 Å, but identical core line shape and energy separation ΔE_{cl} were observed throughout the 10–25 Å thickness range explored. Based on Eq. (1), the variation in the energy separation of the core levels in Fig. 4(b) relative to 4(a) gives directly the valence-band offset. We found $\Delta E_v = +0.07 \pm 0.07$ eV, i.e., the valence-band maximum in CdTe(001) laying 0.07 eV below that of GaAs(001). A similar result ($\Delta E_v = +0.09 \pm 0.07$ eV) was obtained using the Cd 3*d* core levels in place of the Cd 4*d* core levels.

The procedure that we used to determine the valence-band maximum is illustrated for GaAs and CdTe with (001) orientation in the uppermost section and midsection of Fig. 5, respectively. To the left we show the result of a least-squares best fit of the broadened theoretical DOS (solid line) to representative experimental spectra (solid circles) in the region of the leading valence-band edge. The binding energy scale is referred to the spectrometer Fermi level E_F, and the position of the valence-band maxima as derived from the fits are shown by vertical bars. The rightmost section of Fig. 5 illustrates the position of E_v (relative to E_F) in GaAs (top) and in CdTe (midsection) resulting from the least-squares fitting procedure as a function of window size (measured from E_F) for three different values of the broadening. Good consistent fits of the leading valence-band edge could be obtained within about 2 eV of E_F.

The value of the FWHM of the Gaussian broadening function ($\sigma = 0.75 \pm 0.05$ eV) was obtained from the experimental EDC's as explained in Sec. II. The dependence of the fit on the 0.05-eV uncertainty on σ is illus-

trated in the right most section in Fig. 5 for GaAs (top) and CdTe (midsection). The variation of E_v in the crucial plateau range is less than ± 0.03 eV, indicating that the procedure is quite robust provided that one is close enough to the actual experimental broadening.

2. *CdTe(111)-GaAs(001)*

XPS determination of the valence-band offset in CdTe(111)-GaAs(001) heterostructures is complicated by the presence of a non-negligible residual strain (see Table I). In a strained layer material the effect of strain on the position of the core levels is comprised of hydrostatic and uniaxial contributions. The separation between the core level and the centroid of the valence bands at Γ in the Brillouin zone is only influenced by the hydrostatic contribution. The uniaxial component of the distortion removes the valence-band degeneracy and modifies the position of the spin-split band, but does not shift the centroid.[33–35] For pseudomorphic Si layers on GaAs or Ge (+4.1% in-plane strain), for example, Hybertsen[49] calculated the hydrostatic shift as 0.1–0.2 eV. This value, when added to the combined spin-orbit–uniaxial strain splitting of the topmost valence-band relative to the centroid of the valence bands at Γ, yielded a total strain-induced increase in the Si $2p$ core binding energy of 0.4–0.5 eV. An extrapolation of the experimental results for $Si_{1-x}Ge_x$ of Ref. 34 also supported such a strain-induced correction to be core binding energy.[35]

The strain-induced correction to the Cd core binding energy in CdTe(111)-GaAs(001) heterostructures is difficult to evaluate *a priori* because of the inhomogeneous nature of the strain in the (111) plane, as shown in Figs. 2(b) and 3 and in Table I. However, Eq. (1) would become again applicable if it is possible to measure directly the Cd core binding energy relative to E_v in an hypothetical CdTe bulk standard exhibiting a strain similar to that encountered near the interface. The systematics of the measured residual strain versus CdTe thickness in Table I suggests that near the interface, and within the 10–25-Å-thick overlayers used for XPS determination of

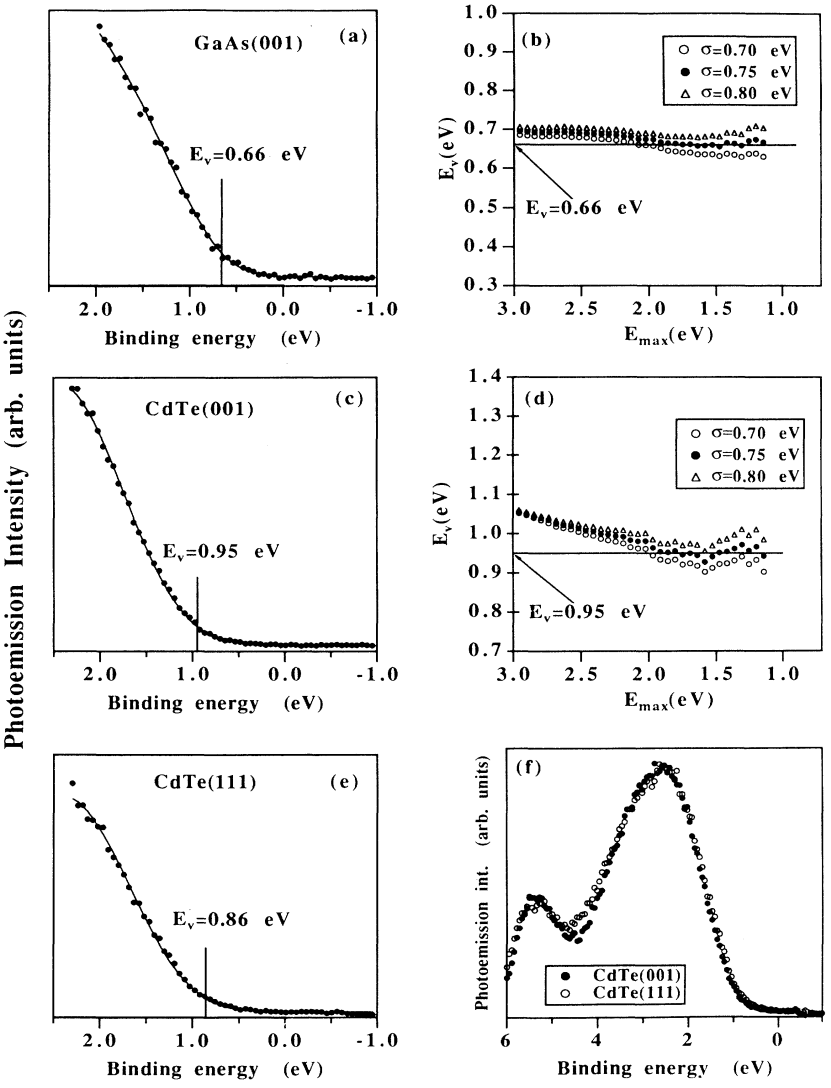

FIG. 5. Determination of the position of the valence-band maximum E_v in MBE-grown epitaxial standards through least-squares fits of the experimental photoemission spectra near the leading valence-band edge to a suitably broadened theoretical density of states (DOS). (a) Best fit (in a 2.3-eV-wide energy window) of the experimental data (solid circles) to the theoretical DOS (from Ref. 36) convoluted (solid line) with a Gaussian instrumental resolution function with full width at half maximum (FWHM) of 0.75 eV. The experimental spectrum was obtained from a 0.5-μm-thick undoped GaAs(001) layer grown at 580 °C. (b) Position of E_v resulting from the fits as a function of the width of the energy window used to evaluate the least-squares deviation. We show results for a Gaussian broadening of the theoretical DOS with FWHM of 0.80 eV (open triangles), 0.75 eV (solid circles), and 0.70 eV (open circles). (c) and (d) Corresponding results for a CdTe(001) standard. The sample was a 5000-Å-thick undoped CdTe(001) layer grown at 290 °C on a GaAs buffer. (c) Best fit (in a 2.3-eV-wide energy window) of the experimental data (solid circles) to the theoretical DOS (from Ref. 36) convoluted (solid line) with a Gaussian function with FWHM of 0.75 eV. (d) Position of E_v resulting from the fit as a function of energy window and experimental resolution. (e) and (f) Results for a 50-Å-thick CdTe(111) standard grown at 290 °C on a GaAs buffer. (e) Best fit (in a 2.3-eV-wide energy window) of the experimental data (solid circles) to the same broadened theoretical DOS used in (c). (f) The experimental leading valence-band edge for the CdTe(111) standard (solid circles) is shown superimposed on that observed for the CdTe(001) standard (open circles).

ΔE_{cl}, the strain is relatively constant and similar to that observed in (111)-oriented CdTe films of thickness ≤ 50 Å. Since at a coverage of 50 Å the thickness of the overlayer exceeds the photoemission sampling depth, the corresponding valence-band emission will involve only CdTe-related contributions.[50] It is therefore possible to use ~50-Å-thick CdTe(111) overlayers to determine directly the strain-corrected value of $E_b - E_v$.

An important point in the derivation of $E_b - E_v$ is the determination of the position of E_v in the strained overlayers. We used two approximate methods with consistent results. First, we performed a linear extrapolation of the leading valence-band edge in the EDC's from (001)- and (111)-oriented standards to extract the correction to the Cd 4*d* binding energy due to the strain. The implied assumption is that despite the strain-induced splitting of the top of the valence band, in a small enough interval near E_v the bands contributing to the DOS are still parabolic enough. We also used the theoretical DOS for bulk, unstrained CdTe to fit the EDC's for (111)-oriented standards in a 2-eV-wide energy window near E_v. This cannot be justified *a priori,* since in principle residual strain will remove the valence-band degeneracy and change the DOS near E_v. The fit should therefore be considered purely as an empirical extrapolation method with no more physical significance than the linear extrapolation method.

The results are shown in the bottom-most section of Fig. 5. In the rightmost panel, we directly compare EDC's for (001)-oriented and strained, (111)-oriented CdTe standards. The zero of the binding energy scale corresponds to the position of the Fermi level in the (111)-oriented standard. The close similarity of the two spectra supports the use of analogous extrapolation methods in a narrow enough energy window near E_v. In the leftmost panel, we compare the experimental valence-band edge for the (111)-oriented standard (solid circles) with the results of the extrapolation method based on the theoretical DOS (solid line). The corresponding position of E_v is marked by a vertical bar.

The determination of the valence-band offset in CdTe(111)-GaAs(001) heterostructures is summarized in Fig. 6. In the leftmost inset, we show EDC's for the valence-band emission from a GaAs(001) standard (bottom) and from a 50-Å-thick CdTe(111) standard (top) grown at 290 °C on GaAs(001). The Ga 3*d* and Cd 4*d* core emission from the same standards is shown in Fig. 6(a). Individual core binding energies were measured relative to the position of E_v in each standard, and the zero of the binding energy scale is shown at the position of the Ga 3*d* centroid in GaAs. From measurements performed on thirteen 50-Å-thick (111)-oriented CdTe standards, we found[51]

$$E_b(\text{Cd } 4d) - E_v(\text{CdTe}) = 10.63 \pm 0.02 \text{ eV} ,$$

$$E_b(\text{Cd } 3d) - E_v(\text{CdTe}) = 404.68 \pm 0.02 \text{ eV} .$$

Such values are larger by about 0.1 eV relative to those observed in fully relaxed (001)-oriented standards. The difference is consistent in direction and order of magnitude with that expected from the presence of residual strain in (111)-oriented thin CdTe overlayers.

The apparent core level separation in Fig. 6(a) is that expected (8.21±0.05 eV) for a hypothetical CdTe(111)-GaAs(001) heterojunction with zero valence-band offset. Using the Cd 3*d* core levels rather than the 4*d* levels, the corresponding core separation (not shown) would be 385.84±0.05 eV.

The Ga 3*d* and Cd 4*d* core emission from an actual

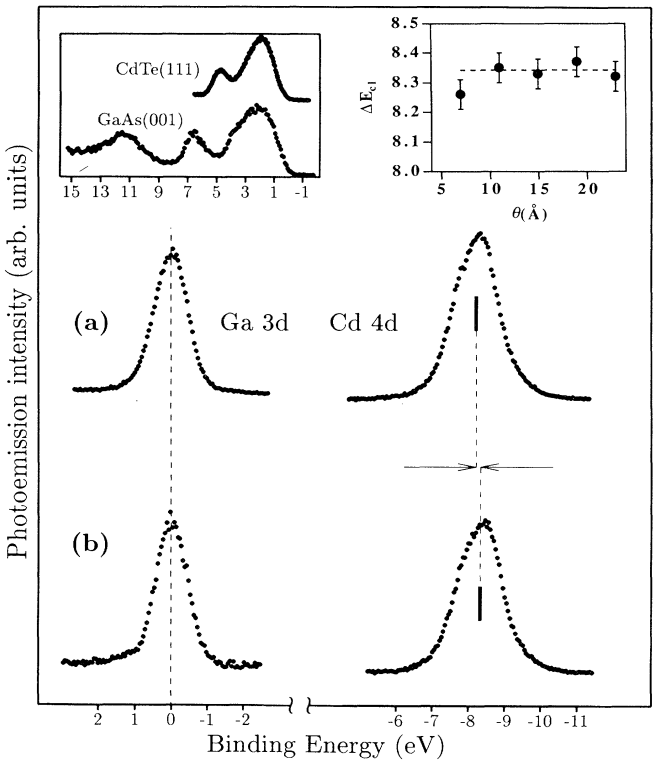

FIG. 6. Leftmost inset: valence-band emission from a 1-μm-thick undoped GaAs(001) 2×4 buffer layer (bottom) grown at 580 °C and from a 50-Å-thick CdTe(111) layer (top) grown at 290 °C on the GaAs buffer. For such a CdTe thickness the maximum in-plane strain is approximately the same as that observed in the ~20-Å-thick overlayers used for photoemission-band offset determination. Rightmost inset: apparent energy separation of the Ga 3*d* and Cd 4*d* core-level emission features from CdTe(111)-GaAs(001) interfaces as a function of CdTe thickness. (a) Ga 3*d* and Cd 4*d* core emission from the same GaAs and CdTe standards used to obtain the valence-band spectra in the leftmost inset. Individual core binding energies were measured relative to the position of E_v in each standard. The zero of the binding-energy scale is shown at the position of the Ga 3*d* centroid in GaAs, so that the apparent core-level separation is that expected in a hypothetical CdTe(111)-GaAs(001) heterojunction with zero valence-band offset. (b) Ga 3*d* and Cd 4*d* core emission from an actual CdTe(111)-GaAs(001) heterojunction fabricated by depositing a 20-Å-thick CdTe(111) layer on GaAs(001). The observed core-level separation is independent of CdTe thickness in the 12–24-Å range explored (rightmost inset) within an uncertainty of ±0.05 eV. The change in core-level separation relative to (a) gives directly the valence-band offset $\Delta E_v = -0.09 \pm 0.07$ eV. A similar value (-0.11 ± 0.07 eV) was obtained using the Cd 3*d* core levels.

CdTe(111)-GaAs(001) heterojunction fabricated by depositing a 20-Å-thick CdTe(111) layer on GaAs(001) is shown in Fig. 6(b). As in the case of CdTe(001)-GaAs(001) heterojunctions, the observed core-level separation (8.30±0.03 eV) is independent of CdTe thickness in the 10–25-Å range, as illustrated in the rightmost inset, within an uncertainty of 0.05 eV. The corresponding Cd $3d$–Ga $3d$ interface core separation (not shown) was 385.73±0.02 eV. In the case of the Cd $4d$–Ga $3d$ cores, $\Delta E_{\rm cl}$ [in Fig. 6(b)] is larger than the bulk energy separation [in Fig. 6(a)], while for the Cd $3d$–Ga $3d$ cores, $\Delta E_{\rm cl}$ is smaller than the bulk energy separation, indicating that the top of the valence band in CdTe(111) lies above that of GaAs(001). The magnitude of the variation in core separation gives directly $\Delta E_v = -0.09$ eV (or -0.11 eV using the Cd $3d$ cores).

We caution the reader that the method used to determine the valence-band maximum in CdTe(111) may limit the accuracy of the above valence-band offsets. In photoemission determinations of the valence-band offset the quoted accuracy (usually much smaller than the experimental energy resolution) rests on our ability to detect *rigid* shifts of core levels and valence-band edge, and therefore on the absence of line shape changes. When strain is applied to a semiconductor, however, the density of states around E_v should change as the degeneracy is removed. The extent to which such a change is detected experimentally may depend on the experimental energy resolution and affect the determination of E_v.

In the absence of substantial changes in the valence-band line shape in Fig. 5(f) when comparing the CdTe(001) and CdTe(111) spectra, it is conceivable that the fit of the leading valence-band edge might be capturing only in part the strain-induced modification of the DOS. If this were the case, then our procedure would *underestimate* the strain-induced change in the valence-band offset relative to the unstrained CdTe(001)-GaAs(001) case. The valence-band offset for the strained CdTe(111)-GaAs(001) interface (-0.09 to -0.11 eV) may carry therefore a somewhat higher uncertainty ($+0.07/-0.12$) as compared to the offset for the unstrained CdTe(001)-GaAs(001) interface.

IV. DISCUSSION

To our knowledge, the only previously published[52,53] study of ΔE_v for CdTe(001)-GaAs(001) heterojunctions was performed by Waag *et al.*,[52] who reported a much larger offset ($+0.47\pm0.08$ eV). These authors also used photoemission data and Eq. (1) to extract the offset. Since the discrepancy between the two values of the offset exceeds the combined experimental uncertainty, a detailed analysis of the procedure leading to the two results is warranted. Differences in two experiments concern the growth procedure of the heterostructure and the data analysis. CdTe deposition in Ref. 52 was performed either at 290 °C or while continuously cooling the substrate from 650 °C to 300 °C, on etched and deoxidized GaAs(001) wafers with unspecified surface reconstruction. For the data analysis, since an unmonochromatized x-ray source was employed,[52] a deconvolution of the valence-band spectra was required to eliminate Mg $K\alpha$ satellite-related contributions and determine E_v.

As far as the data analysis is concerned, the difference in the numerical value of the offset reflects differences in both the interface core separation $\Delta E_{\rm cl}$ and the position of the core levels in bulk standards [see Eq. (1)]. In our study, the average value of the Ga $3d$–Cd $4d$ energy separation $\Delta E_{\rm cl}$ from 16 heterostructures was 8.22 eV,[54] with a standard deviation of only 0.03 eV. The Ga $3d$–Cd $4d$ interface core separation from the same samples was 385.84±0.03 eV, leading to a valence-band offset from Eq. (1) virtually identical to that obtained using the shallower Cd core levels ($\Delta E_v = +0.09\pm0.07$ as compared to the previous value of $+0.07\pm0.07$ eV). In Ref. 52 measurements for five different heterostructures yielded a Ga $3d$–Cd $4d$ core separation of 8.09±0.03 eV.[55] Since the difference in experimental energy resolution (0.75 eV in our work as compared to 1.1 eV in Ref. 52) should not affect substantially $\Delta E_{\rm cl}$, a sensibly different interface core separation was observed in the two experiments as a result of differences in the growth procedure. Unfortunately, since no structural information was provided in Ref. 52, we cannot speculate at this time on differences in interface atomic structure or composition that might explain this result.

The determination of the core binding energies from bulk standards has two major sources of uncertainty, namely possible differences in residual strain for the bulk standards and the thin films used in the heterojunction studies, and the determination of the position of the valence-band maximum E_v in the valence-band EDC's. The former does not play a role in our CdTe(001)-GaAs(001) result, since both the RHEED and XTEM results support a fully relaxed nature of the overlayers even at the lowest coverages explored. The latter has been determined in our results through a least-squares fit of the leading valence-band edge to suitably broadened theoretical DOS for CdTe and GaAs,[36] while in Ref. 52 a linear extrapolation of the same valence-band edge was employed, after removal of the Mg $K\alpha$ satellite feature from the CdTe valence band.

The core-level binding energies quoted in Ref. 52 are E_b(Ga $3d$) $-E$(GaAs) $=19.26\pm0.05$ eV and E_b(Cd $4d$) $-E_v$(CdTe) $=10.69\pm0.05$ eV. The comparison suggests that the linear extrapolation method yields a systematic error of different magnitude when estimating the position of E_v in GaAs and CdTe. This is not unexpected since cancellation of systematic errors due to the linear extrapolation method can be reasonably expected only for very similar valence-band DOS, as those encountered in common anion systems.[16,37,38] We conclude that of the 0.4-eV difference between the values of ΔE_v found here (0.07–0.09 eV) and that reported in Ref. 52 (0.47 eV) for CdTe(001)-GaAs(001) heterojunctions, about one-third (0.14 eV) is due to an actual difference in core-level separation at the interface, and two-thirds (0.26 eV) to the difference in the position of the valence-band maxima in the bulk standards. We speculate that a possible contribution to the discrepancy stems from the deconvolution procedure indispensable in the results of Waag *et al.* to

subtract the satellite contribution to the CdTe valence band. Such a subtraction is bound to degrade the signal-to-noise ratio and increase the experimental uncertainty of the offset.

In the literature, the Ga 3*d* position relative to E_v in (001)-oriented bulk GaAs standards has been reported as 18.73±0.05 eV,[56] 18.75±0.03 eV,[57] 18.78±0.03 eV,[23] and 18.83±0.05 eV.[58] Within experimental uncertainty, most of these results are quite similar to ours. The situation is less clear for CdTe. XPS investigations have only examined, to our knowledge, CdTe($\overline{111}$) standards. Kowalczyk *et al.* reported a Cd 4*d* centroid position 10.293±0.03 eV below E_v for CdTe buffer layers grown at 265 °C on CdTe($\overline{111}$) wafers,[37] while Duc, Hsu, and Faurie[59] obtained a 10.145±0.03 eV peak position of the Cd $4d_{5/2}$ spin-split subcomponent (a linear extrapolation was used to determine E_v) in similar samples grown at 190 °C. Such values seem inconsistent with those obtained here from measurements of eleven (001)-oriented CdTe standards (see, however, Ref. 53). At XPS energies, surface-related effects should have little influence on the measured core binding energies.[60] Comparison of Cd 4*d* spectra recorded from 0.6-μm-thick CdTe(001) standards, 50-Å-thick CdTe(111) standards, and the corresponding 15-Å-thick CdTe layers showed that the line shape of the core levels remained unchanged, as expected in the absence of surface-related contribution, so that the discrepancy remains unexplained.

The difference between the valence-band discontinuities observed in CdTe(001)-GaAs(001) and CdTe(111)-GaAs(001) interfaces may in principle reflect differences in local atomic configuration at the interface, difference in strain, or both. An attempt to discriminate between the effect of local interface environment and residual strain has to rely in part on additional theoretical and experimental information. Recent linear-response theory arguments have shown that in heterovalent semiconductor interfaces with polar orientation the band offsets may in principle be affected by the detail of the interface atomic structure.[7,11] This is in sharp contrast with the behavior of isovalent heterojunctions, for which the band offset should be a bulk property of the two materials comprising the junction. Heterovalent heterojunctions with nonpolar orientation should exhibit a behavior similar to that of isovalent heterojunctions, with band offsets independent of the atomic structure of the interface.

To our knowledge, the only available results about CdTe-GaAs interfaces with nonpolar orientation is a recent synchrotron radiation photoemission study[61] of heterojunctions fabricated through room-temperature growth of amorphous CdTe layers on GaAs substrates cleaved *in situ*. As in the present study, a single compound effusion cell was used for CdTe deposition. The resulting αCdTe-GaAs(110) interfaces exhibited a valence-band offset of +0.20±0.05 eV.

Using here for simplicity the average values of the offsets obtained from the Cd 4*d* and Cd 3*d* core levels, we see that for αCdTe-GaAs(001) ($\Delta E_v = +0.20$ eV) and CdTe(001)-GaAs(001) interfaces ($\Delta E_v = +0.08$ eV), which involve both fully relaxed CdTe overlayers, the measured band offsets are surprisingly similar to the predictions of a number of simple linear theories of heterojunction band discontinuities, such as Anderson's model ($\Delta E_v = +0.22$ eV, Ref. 62), the empirical deep-level model ($\Delta E_v = +0.23$ eV, Ref. 63), and Harrison's tight-binding model ($\Delta E_v = +0.21$ eV, Ref. 64). More sophisticated calculations, by Tersoff ($\Delta E_v = +0.35$ eV, Ref. 9) and Van de Walle and Martin ($\Delta E_v = -0.05$ eV, Ref. 5), predict slightly different values.

For CdTe(111)-GaAs(001) interfaces, which exhibit an appreciably different offset ($\Delta E_v = -0.10$ eV), the possible contribution of residual strain can be estimated along the lines proposed by Van de Walle.[17] Deformation potentials in the linear approximation are used to describe the effects of strain on the electronic bands, the zero-order lineup being obtained from one or the other of the linear models of heterojunction behavior. Unfortunately, in view of the inhomogeneous strain configuration in the (111) plane, the expressions for stress fields with tetragonal symmetry in Ref. 17 are not appropriate for CdTe(111)-GaAs(001) heterojunctions. For a rough estimate of the magnitude of the strain-related correction, we used expressions[17] appropriate for an unstrained GaAs(001) substrate and a tetragonally distorted CdTe(111) overlayer with a homogeneous in-plane strain of 2% (see Table I). The shift of the center of mass of the valence bands due to the hydrostatic component of the strain, together with the strain-induced splitting of the top of the valence bands, results in an upward shift of the valence-band maximum in CdTe of the order of 0.1 eV relative to the unstrained case. The expected variation in valence-band offset is therefore consistent in sign and order of magnitude with that observed in comparing CdTe(111)-GaAs(001) and CdTe(001)-GaAs(001) interfaces. We cannot rule out, however, an additional role of the different interface atomic structure in determining the observed difference in offset.

V. CONCLUSIONS

Molecular-beam epitaxy of CdTe overlayers and GaAs substrates was employed to synthesize CdTe(001)-GaAs(001) and CdTe(111)-GaAs(001) heterostructures while maximizing long-range order within the interface region. Cross-sectional transmission electron microscopy studies of the interface atomic structure revealed a fully relaxed CdTe overlayer in CdTe(001)-GaAs(001) heterostructures and a well-defined residual strain gradient extending ~200 Å into the overlayer for CdTe(111)-CdTe(001) heterostructures. Comparison with grazing incidence x-ray diffraction results suggests that the gradual strain relaxation observed as a function of coverage in thin CdTe(111) films on GaAs is similar to the residual strain gradient observed near the buried interface in macroscopic CdTe(111)-GaAs(001) heterostructures.

Monochromatic x-ray photoemission measurements of the valence-band offsets in the two heterostructures showed a valence-band offset of +0.08 eV for CdTe(001)-GaAs(001) interfaces and a valence-band offset of −0.10 eV for CdTe(111)-GaAs(001) interfaces, to be compared with the value of +0.20 eV reported earlier for fully relaxed αCdTe-GaAs(110) interfaces. We find therefore that residual strain may be sufficient to ex-

plain most of the observed difference in band offsets between CdTe(001)-GaAs(001) and CdTe(111)-GaAs(001) interfaces, although the different interface atomic structure may also play a role, more difficult to quantify at this stage due to the lack of a suitable theoretical model for the electronic structure of the two interfaces.

ACKNOWLEDGMENTS

The work of Minnesota was supported by the U.S. Army Research Office, under Grants Nos. DAAL03-90-G-0001 and DAAH04-93-G-0206, and by the Center for Interfacial Engineering at the University of Minnesota, under Grant No. NSF-CDR 8721551. One of us (G.B.) would like to acknowledge the support of the Consorzio dell' Area di Ricerca di Trieste. We thank S. Baroni, J. P. Faurie, R. W. Grant, M. S. Hybertsen, M. Peressi, R. Resta, G. P. Schwartz, and C. G. Van de Walle for useful discussions or for providing us with the results of their work prior to publication.

---

*On leave from Istituto di Acustica O. M. Corbino del CNR, Via Cassia 1216, I-00189 Roma, Italy.

[1]S. Tatarenko, J. Cibert, Y. Gobil, G. Feuillet, K. Saminadayar, A. C. Chami, and E. Ligeon, Appl. Surf. Sci. **41/42**, 470 (1989).

[2]R. H. Feldman, R. F. Austin, D. W. Kisker, R. S. Jeffers, and P. M. Brindenbach, Appl. Phys. Lett. **48**, 248 (1986), and references therein.

[3]J. M. DePuydt, M. A. Haase, J. Qiu, and H. Cheng, J. Cryst. Growth **117**, 1078 (1992).

[4]L. Vanzetti, A. Rasanen, L. Sorba, X. Yu, G. Haugstad, G. Bratina, and A. Franciosi, J. Cryst. Growth **117**, 573 (1992).

[5]C. G. Van de Walle and R. M. Martin, Phys. Rev. B **35**, 8154 (1987); **37**, 4801 (1988).

[6]M. Cardona and N. E. Christiensen, Phys. Rev. B **35**, 6182 (1987); N. E. Christiensen, *ibid.*, **37**, 4528 (1988).

[7]S. Baroni, R. Resta, and A. Baldereschi, in *Spectroscopy of Semiconductor Microstructures,* Vol. 206 of *NATO Advanced Study Institute, Series B: Physics,* edited by G. Fasol, A. Fasolino, and P. Lugli (Plenum, New York, 1989), p. 251, and references therein; M. Peressi, S. Baroni, R. Resta, and A. Baldereschi, Phys. Rev. B **43**, 7347 (1991).

[8]W. A. Harrison, J. Vac. Sci. Technol. **16**, 1492 (1979).

[9]J. Tersoff, J. Vac. Sci. Technol. B **4**, 1066 (1986).

[10]R. Kunc and R. M. Martin, Phys. Rev. B **24**, 3445 (1981).

[11]S. Baroni, R. Resta and A. Baldereschi, in *Proceedings of the 19th International Conference on the Physics of Semiconductors,* edited by W. Zawadski (IOP, Polish Academy of Sciences, Wroclaw, 1988), p. 525.

[12]L. Sorba, G. Bratina, G. Ceccone, A. Antonini, J. F. Walker, M. Micovic, and A. Franciosi, Phys. Rev. B **43**, 2450 (1991); G. Bratina, L. Sorba, A. Antonini, G. Biasiol, and A. Franciosi, *ibid.* **45**, 4528 (1992), and references therein.

[13]See, for example, F. Capasso, Mater. Res. Soc. Bull. **16**, 23 (1991).

[14]A. Muñoz, N. Chetty, and R. M. Martin, Phys. Rev. B **41**, 2976 (1990).

[15]J. T. McKinley, Y. Hwu, B. E. C. Koltenbach, G. Margaritondo, S. Baroni, and R. Resta, J. Vac. Sci. Technol. A **9**, 917 (1991); M. Marsi, S. La Rosa, Y. Hwu, F. Gozzo, C. Coluzza, A. Baldereschi, G. Margaritondo, J. T. McKinley, S. Baroni, and R. Resta, J. Appl. Phys. **71**, 2048 (1992).

[16]L. Sorba, G. Bratina, A. Antonini, A. Franciosi, L. Tapfer, A. Migliori, and P. Merli, Phys. Rev. B **46**, 6834 (1992); G. Biasiol, L. Sorba, G. Bratina, R. Nicolini, A. Franciosi, M. Peressi, S. Baroni, R. Resta, and A. Baldereschi, Phys. Rev. Lett. **69**, 1283 (1992), and references therein.

[17]C. G. Van de Walle, Phys. Rev. B **39**, 1871 (1989).

[18]H. A. Mar, N. Salansky, and K. T. Chee, Appl. Phys. Lett. **44**, 898 (1984).

[19]G. Cohen-Solal, F. Bailly, and M. Barbe, Appl. Phys. Lett. **49**, 1519 (1986); E. Ligeon, C. Chami, R. Danielou, G. Feuillet, J. Fontenille, K. Saminadayar, A. Ponchet, J. Cibert, Y. Gobil, and S. Tatarenko, J. Appl. Phys. **67**, 2428 (1990).

[20]F. A. Ponce, G. B. Anderson, and J. M. Ballingall, Surf. Sci. **168**, 564 (1986).

[21]N. Otsuka, L. A. Kolodziejski, R. L. Gunshor, S. Datta, R. N. Bicknell, and J. F. Schetzina, Appl. Phys. Lett. **46**, 860 (1985).

[22]R. G. Dandrea, S. Froyen, and A. Zunger, Phys. Rev. B **42**, 3213 (1990).

[23]In the photoelectron kinetic-energy range of interest here E. A. Kraut, R. W. Grant, J. R. Waldrop, and S. P. Kowalczyk, Phys. Rev. B **28**, 1965 (1983), determined the escape depth as 26.6 Å for normally emitted electrons.

[24]S. Tatarenko, K. Saminadayar, J. Cibert, Y. Gobil, G. Cohen-Solal, and F. Bailly, Proc. SPIE **944**, 2 (1988).

[25]Various types of 6×1 RHEED patterns have been observed for CdTe-GaAs, depending on Te flux and substrate temperature. They differ in the shape of $\frac{1}{6}$ order streaks and the amount of adsorbed Te, which can be less or more than one monolayer.

[26]M. A. Herman and H. Sitter, *Molecular Beam Epitaxy, Fundamentals and Current Status,* Springer Series in Materials Science Vol. 7 (Springer, Berlin, 1989).

[27]See G. Feuillet, in *Evaluation of Advanced Semiconductor Materials by Electron Microscopy,* Proceedings of the NATO Advanced Research Workshop, edited by D. Cheris (Plenum, New York, 1989), p. 33.

[28]See, for example, L. J. Brillson, in *Handbook on Semiconductors,* 2nd ed., edited by P. T. Landsberg (Elsevier, Amsterdam, 1992), Vol. 1, Chap. 8.

[29]RHEED oscillations could not be detected during the early CdTe(001) growth stage on GaAs substrates.

[30]See, for example, *Heterojunctions Band Discontinuities: Physics and Device Applications,* edited by F. Capasso and G. Margaritondo (North-Holland, Amsterdam, 1987).

[31]The sign of the valence-band offset is taken here as positive when the valence-band maximum in the substrate is *above* that of the overlayer.

[32]J. Tersoff and C. G. Van de Walle, Phys. Rev. Lett. **59**, 946 (1987).

[33]G. P. Schwartz, M. S. Hybertsen, J. Bevk, R. G. Nuzzo, J. P. Mannaerts, and G. J. Gualtieri, Phys. Rev. B **39**, 1235 (1989).

[34]E. T. Yu, E. T. Croke, D. H. Chow, D. A. Collins, M. C. Phillips, T. C. McGill, J. O. McCaldin, and R. H. Miles, J. Vac. Sci. Technol. B **8**, 908 (1990).

[35]G. Bratina, L. Sorba, A. Antonini, L. Vanzetti, and A. Franciosi, J. Vac. Sci. Technol. B **9**, 2225 (1991).

[36]J. R. Chelikowsky and M. L. Cohen, Phys. Rev. B **14**, 556 (1976).

[37]S. P. Kowalczyk, J. T. Cheung, E. A. Kraut, and R. W. Grant, Phys. Rev. Lett. **56**, 1605 (1986).

[38]S. P. Kowalczyk, E. A. Kraut, J. R. Waldrop, and R. W. Grant, J. Vac. Sci. Technol. **21**, 482 (1982).

[39]P. H. Citrin, G. K. Wertheim, and Y. Baer, Phys. Rev. Lett. **41**, 1425 (1978).

[40]V. H. Etgens, R. Pinchaux, M. Sauvage-Simkin, J. Massies, N. Jedercy, N. Geiser, and S. Tatarenko, Surf. Sci. **251/252**, 478 (1991).

[41]R. D. Feldman and R. F. Austin, Appl. Phys. Lett. **49**, 954 (1986).

[42]G. Cohen-Solal, F. Bailly, and M. Barbé, Appl. Phys. Lett. **49**, 1519 (1986).

[43]J. E. Angelo, W. W. Gerberich, G. Bratina, L. Sorba, and A. Franciosi, J. Cryst. Growth (to be published).

[44]The slightly different growth protocol employed for the samples in Figs. 1(c), and 1(d) relative to procedure II involved a GaAs(001) $c(4\times4)$ surface heated at 320 °C under Te flux prior to CdTe growth at 290 °C.

[45]Our RHEED instrument was not optimized for quantitative measurements of the lattice parameters. Small differences in streak separation may occur due to the different sample positioning relative to the screen and the camera, and are not meaningful.

[46]G. Patrat, E. Soyez, M. Brunel, J. Cibert, S. Tatarenko, and K. Saminadayar, Solid State Commun. **74**, 433 (1990). More recent results for the nominal 20-Å CdTe(111) layer on GaAs show a residual strain of 2% in the $[1\bar{1}0]$ direction, i.e., closer to our XTEM values. See A. Bourret, P. Fuoss, G. Feuillet, and S. Tatarenko, Phys. Rev. Lett. **70**, 311 (1993).

[47]A. Wall, Y. Gao, A. Raisanen, A. Franciosi, and J. R. Chelikowsky, Phys. Rev. B **43**, 4988 (1991).

[48]The Cd 4*d* binding energies with respect to the valence-band maxima obtained by the linear extrapolation of the leading edge of the valence-band emission in CdTe(001) were systematically 0.07 eV lower in energy than in the case of valence-band maxima obtained by the DOS fitting procedure.

[49]M. S. Hybertsen, in Ref. 33 and private communication.

[50]At a CdTe coverage of 50 Å, the contribution of the GaAs substrate to the overall valence-band photoemission intensity, keeping into account the experimental relative XPS cross section, was $\leq 4\%$.

[51]The Cd 4*d* binding energies with respect to the valence-band maxima obtained by the linear extrapolation of the leading edge of the valence-band emission in CdTe(111) were systematically 0.04 eV lower in energy than in the case of valence-band maxima obtained by the DOS fitting procedure.

[52]A. Waag, Y. S. Wu, R. N. Bicknell-Tassius, C. Gonser-Buntrock, and G. Landwehr, J. Appl. Phys. **68**, 212 (1990).

[53]Unpublished results by Faurie and co-workers, however, also support a lower value for the CdTe-GaAs valence-band offset, J. P. Faurie (private communication).

[54]Line-shape centroids were used in all estimates of core positions and separations.

[55]The averages values in Ref. 52 have been recalculated here using our convention that a single heterostructure should contribute a single offset value to the average.

[56]E. T. Yu, D. H. Chow, and T. C. McGill, J. Vac. Sci. Technol. B **7**, 391 (1989).

[57]J. R. Waldrop, R. W. Grant, and E. A. Kraut, J. Vac. Sci. Technol. B **5**, 1209 (1987).

[58]Y. Hashimoto, K. Hirakawa, and T. Ikoma, Appl. Phys. Lett. **57**, 2555 (1990).

[59]T. M Duc, C. Hsu, and J. P. Faurie, Phys. Rev. Lett. **58**, 1127 (1987).

[60]In the comparison with the literature, we emphasized XPS results that are least affected by surface- and matrix-element-related effects. At photon energies in the 50–90-eV range P. John, T. Miller, T. C. Hsieh, A. P. Saphiro, A. L. Wachs, and T.-C. Chiang, Phys. Rev. B **34**, 6704 (1986), reported a value of 10.13 eV for the bulk-related Cd $4d_{5/2}$ feature in Ar^+ sputtered CdTe(001) samples. For (110)-oriented samples H. Höchst, D. Niles, and I. Hernandez-Calderon, Phys. Rev. B **40**, 8370 (1989), obtained a value of 9.95 eV for the Cd $4d_{5/2}$ feture, while Wall *et al.* (Ref. 50) reported a value of 10.10 eV.

[61]X. Yu, A. Raisanen, G.Haugstad, G. Ceccone, N. Troullier, and A. Franciosi, Phys. Rev. B **42**, 1872 (1990).

[62]R. L. Anderson, Solid State Electron. **5**, 541 (1962).

[63]J. M. Langer and H. Heinrich, Phys. Rev. Lett. **55**, 1414 (1985); Physica B+C **134**, 444 (1985).

[64]W. A. Harrison, J. Vac. Sci. Technol. **14**, 1016 (1977).

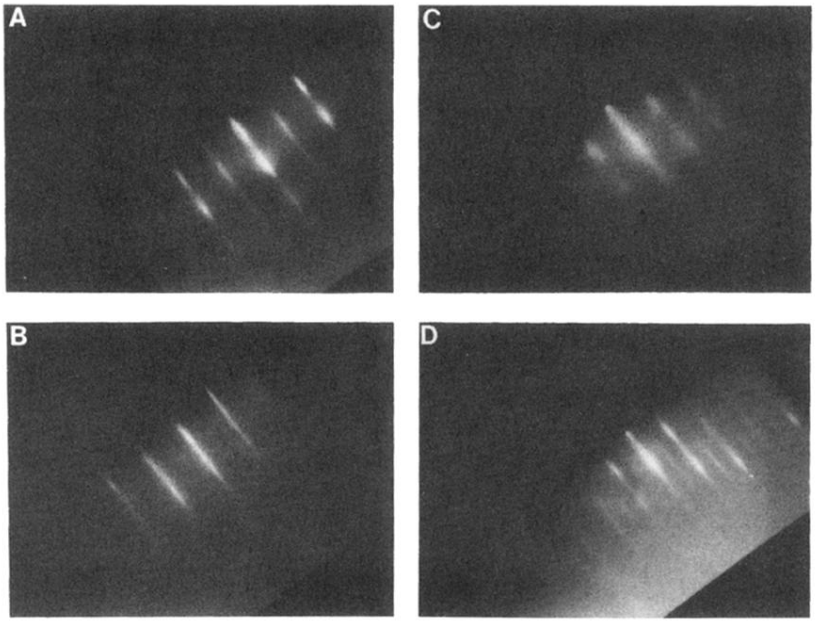

FIG. 1. (a) Reflection high-energy electron diffraction (RHEED) pattern at 10 keV from a 13-Å-thick CdTe(111) epitaxial layer grown by molecular-beam epitaxy (MBE) at 330 °C on a 1-μm-thick undoped GaAs(001) 2×4 buffer layer. The GaAs buffer was grown by MBE at 580 °C on GaAs(001). Azimuth: [$1\bar{1}0$]GaAs. (b) RHEED pattern from a 0.6-μm-thick CdTe(111) epitaxial layer grown in the same conditions as in (a). (c) RHEED pattern from a 14-Å-thick CdTe(001) epitaxial layer grown at 330 °C on a GaAs(001) wafer after oxide desorption at 580 °C and exposure to a suitable Te flux. Azimuth: [110]GaAs. (d) RHEED pattern for a 0.6-μm-thick CdTe(001) epitaxial layer grown in the same conditions as in (c).

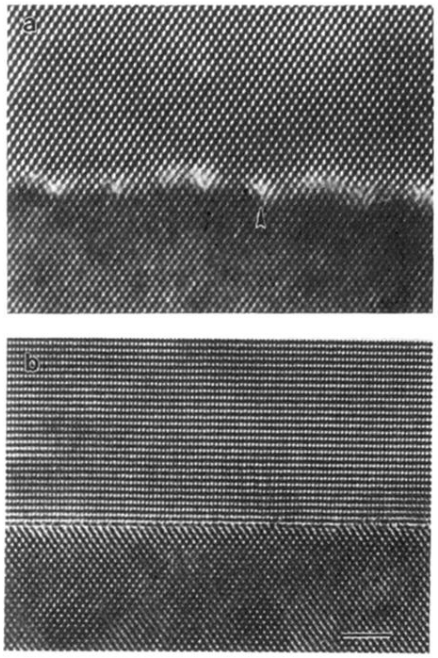

FIG. 2. High-resolution transmission electron micrographs of the interface region within CdTe-GaAs heterostructures, imaged along the [110] direction of GaAs. The length of the horizontal marker (horizontal bar, lower photograph) corresponds to 25 Å. The topmost section of each photograph corresponds to the MBE-grown CdTe overlayer, the bottom-most section of the MBE-grown GaAs substrate. (a) CdTe(001)-GaAs(001) heterostructure, viewed along $[1\bar{1}0]$CdTe||[110]GaAs. The overlayer is fully relaxed and the 14.6% mismatch is accommodated through the formation of a network of misfit dislocations spaced 32 Å apart along the interface. The vertical arrow marks the position of the core of one such dislocation. (b) CdTe(111)-GaAs(001) heterostructure, viewed along $[11\bar{2}]$CdTe ||[110]GaAs. The overlayer in-plain strain configuration is inhomogeneous, in view of the -14.6% mismatch along $[1\bar{1}0]$CdTe||$[1\bar{1}0]$GaAs and the $+0.65\%$ mismatch along $[11\bar{2}]$CdTe||[110]GaAs.

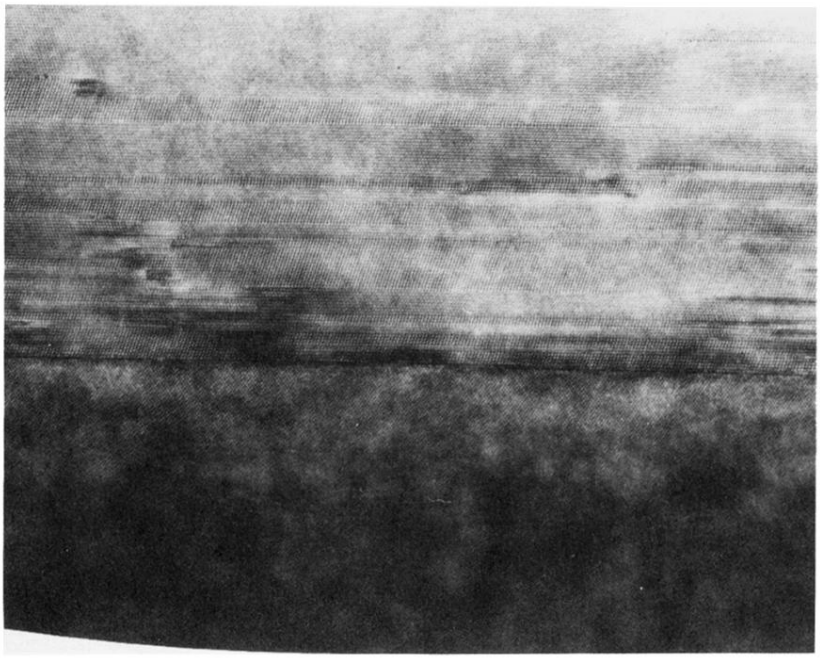

FIG. 3. Lower magnification high-resolution transmission electron micrograph of CdTe(111)-GaAs(001) heterostructure showing extended regions of substrate and overlayer along $[1\bar{1}0]$CdTe$||[1\bar{1}0]$GaAs. A distribution of rotational twins in the $[11\bar{2}]$CdTe$||$[110]GaAs direction gradually accommodates the residual strains at the interface.